

Dispersive analysis of the $\gamma^*\gamma^* \rightarrow \pi\pi$ process

Igor Danilkin,^{1,*} Oleksandra Deineka,¹ and Marc Vanderhaeghen¹

¹*Institut für Kernphysik & PRISMA⁺ Cluster of Excellence,
Johannes Gutenberg Universität, D-55099 Mainz, Germany*

(Dated: March 19, 2020)

We present a dispersive analysis of the double-virtual photon-photon scattering to two pions up to 1.5 GeV. Through unitarity, this process is very sensitive to hadronic final-state interaction. For the s -wave, we use a coupled-channel $\pi\pi$, $K\bar{K}$ analysis which allows a simultaneous description of both $f_0(500)$ and $f_0(980)$ resonances. For higher energies, $f_2(1270)$ shows up as a dominant structure which we approximate by a single-channel $\pi\pi$ rescattering in the d -wave. In the dispersive approach, the latter requires taking into account t - and u -channel vector-meson exchange left-hand cuts which exhibit an anomalous-like behavior for large space-like virtualities. We show how to readily incorporate such behavior using a contour deformation. Besides, we devote special attention to kinematic constraints of helicity amplitudes and show their correlations explicitly.

I. INTRODUCTION

It is still an open question whether a current ultra-precise $(g-2)_\mu$ measurement can probe the physics beyond the Standard Model. The presently observed $3-4\sigma$ deviation between theory [1–3] and experiment [4] has a potential to become more significant once results from new measurements at both FERMILAB [5] and J-PARC [6] are available. On the other hand, the current theoretical error results entirely from hadronic contributions. The hadronic uncertainties mainly originate from the hadronic vacuum polarization (HVP) and the hadronic light-by-light (HLbL) processes. Forthcoming data from the high luminosity e^+e^- colliders, in particular, from the BESIII and Belle-II Collaborations will further reduce the uncertainty in the HVP in the coming years to make it commensurate with the experimental precision on $(g-2)_\mu$. The remaining hadronic uncertainty results from HLbL, where, apart from the pseudo-scalar pole contribution, a further nontrivial contribution comes from the two-particle intermediate states such as $\pi\pi$, $\pi\eta$ and $K\bar{K}$.

The rescattering of $\pi\pi$ and $\pi\eta$ is responsible for the contribution from $f_0(500)$, $f_0(980)$, $f_2(1270)$, and $a_0(980)$, which can be taken into account in a dispersive framework. Among them, only $f_2(1270)$ can be interpreted within the quark model as a state that does not originate from long-range interactions [7]. Given the fact that it is relatively narrow, its contribution to $(g-2)_\mu$ can be accounted for in two ways: by using a pole contribution as it is given in [8] (updated in [9] using recent data from the Belle Collaboration [10]) or through fully dispersive formalisms [11] and [12] with input from $\gamma^*\gamma^* \rightarrow \pi\pi$. The comparison will shed light on the effective resonance description of other resonances such as axial-vector contributions [1, 8].

In this paper, we present an analysis of the double vir-

tual photon fusion reaction with pions in the final state. Our approach relies on the modified Muskhelishvili-Omnès formalism, which proves to be efficient in the description of the real photon data [13]. Within the maximal analyticity assumption [14], all of the non-analytic behavior of the amplitude should be coming from the unitarity and crossing symmetry constraints. Therefore in order to write the dispersion-integral representation for the partial wave helicity amplitudes, one needs to make sure that they are free from kinematic constraints at thresholds or pseudo-thresholds. The critical step in finding these constraints is the decomposition of the amplitude into Lorentz structures and invariant amplitudes [15]. The latter are expected to satisfy the Mandelstam dispersion-integral representation [16]. Once a suitable set of Lorentz structures is found, the rest is straightforward. Our work is a continuation of a previous work where, for the first time, the single virtual case for the d -wave has been studied [17]. In the double virtual photon case, there is an additional complication related to the anomalous threshold behavior, as was pointed out in [18]. We will show an alternative way of taking this contribution into account using an appropriate contour deformation.

II. FORMALISM

A. Kinematic constraints

The two-photon fusion reaction $\gamma^*\gamma^* \rightarrow \pi\pi$ is a subprocess of the unpolarized double tagged process $e^+(k_1)e^-(k_2) \rightarrow e^+(k'_1)e^+(k'_2)\pi(p_1)\pi(p_2)$ which is given (in Lorenz gauge) as

$$i\mathcal{M} = \frac{ie^2}{q_1^2 q_2^2} [\bar{v}(k_1)\gamma_\mu v(k'_1)] [\bar{u}(k'_2)\gamma_\nu u(k_2)] H^{\mu\nu}, \quad (1)$$

$$H^{\mu\nu} = i \int d^4x e^{-iq_1 \cdot x} \langle \pi(p_1)\pi(p_2) | T(j_{em}^\mu(x) j_{em}^\nu(0)) | 0 \rangle,$$

with $q_1 \equiv k_1 - k'_1$, where the momenta of leptons k'_1 and k'_2 are detected. This corresponds to the kinematical

*Electronic address: danilkin@uni-mainz.de

situation where photons with momenta q_1 and q_2 have finite space-like virtualities, $q_1^2 = -Q_1^2$ and $q_2^2 = -Q_2^2$. By contracting the hadronic tensor $H^{\mu\nu}$ with polarization vectors, one defines helicity amplitudes $H_{\lambda_1\lambda_2}$ which can be further decomposed into partial waves

$$\begin{aligned} \epsilon_\mu(q_1, \lambda_1) \epsilon_\nu(q_2, \lambda_2) H^{\mu\nu} &\equiv e^{i\phi(\lambda_1-\lambda_2)} H_{\lambda_1\lambda_2} \\ &= e^{i\phi(\lambda_1-\lambda_2)} N \sum_{J \text{ even}} (2J+1) h_{\lambda_1\lambda_2}^{(J)}(s) d_{\Lambda,0}^{(J)}(\theta), \end{aligned} \quad (2)$$

where $\Lambda = \lambda_1 - \lambda_2$, $d_{\Lambda,0}^{(J)}(\theta)$ is a Wigner rotation function and θ is the c.m. scattering angle. In Eq. (2), $N = 1$ for $\gamma^*\gamma^* \rightarrow \pi\pi$ and $N = 1/\sqrt{2}$ for $\gamma^*\gamma^* \rightarrow K\bar{K}$, ensuring the same unitarity relations for the identical and non-identical particles in the case of $I = 0$.

It is well known that partial wave (p.w.) amplitudes $h_{\lambda_1\lambda_2}^{(J)}$ may have kinematic singularities or may obey kinematic constraints [19, 20]. Therefore, it is important to find a transformation to a new set of amplitudes which are more appropriate to use in partial-wave dispersion relations. The key step is to decompose the scattering amplitude into a complete set of invariant amplitudes [15] (see also [21])

$$H^{\mu\nu} = \sum_{i=1}^5 F_i L_i^{\mu\nu}, \quad (3)$$

where

$$\begin{aligned} L_1^{\mu\nu} &= q_1^\nu q_2^\mu - (q_1, q_2) g^{\mu\nu}, \\ L_2^{\mu\nu} &= (\Delta^2 (q_1, q_2) - 2 (q_1, \Delta) (q_2, \Delta)) g^{\mu\nu} - \Delta^2 q_1^\nu q_2^\mu \\ &\quad - 2 (q_1, q_2) \Delta^\mu \Delta^\nu + 2 (q_2, \Delta) q_1^\mu \Delta^\nu + 2 (q_1, \Delta) q_2^\mu \Delta^\nu, \\ L_3^{\mu\nu} &= (t-u) \left\{ (Q_1^2 (q_2, \Delta) - Q_2^2 (q_1, \Delta)) \left(g^{\mu\nu} - \frac{q_1^\nu q_2^\mu}{(q_1, q_2)} \right) \right. \\ &\quad - \left(\Delta^\nu - \frac{(q_2, \Delta) q_1^\nu}{(q_1, q_2)} \right) (Q_1^2 q_2^\mu + q_1^\mu (q_1, q_2)) \\ &\quad \left. + \left(\Delta^\mu - \frac{(q_1, \Delta) q_2^\mu}{(q_1, q_2)} \right) (Q_2^2 q_1^\nu + q_2^\nu (q_1, q_2)) \right\}, \\ L_4^{\mu\nu} &= Q_1^2 Q_2^2 g^{\mu\nu} + Q_1^2 q_2^\mu q_2^\nu + Q_2^2 q_1^\mu q_1^\nu + q_1^\mu q_2^\nu (q_1, q_2), \\ L_5^{\mu\nu} &= (Q_1^2 \Delta^\mu + (q_1, \Delta) q_1^\mu) (Q_2^2 \Delta^\nu + (q_2, \Delta) q_2^\nu), \end{aligned} \quad (4)$$

where $\Delta \equiv p_1 - p_2$ and each $L_i^{\mu\nu}$ satisfies a gauge invariance constraint, i.e., $q_{1\mu} L_i^{\mu\nu} = q_{2\nu} L_i^{\mu\nu} = 0$. The numbering of the Lorentz structures is chosen such that in the single virtual case only $L_{1,2,3}^{\mu\nu}$ contribute to the process [17], while in the real photon case, only $L_{1,2}^{\mu\nu}$ are relevant, which coincide with the tensor structures used in [22, 23]. The invariant amplitudes F_i are free from kinematic singularities or constraints and depend on the Mandelstam variables, which we choose as $s = (q_1 + q_2)^2$, $t = (p_1 - q_1)^2$, and $u = (p_1 - q_2)^2$. The prefactor $(t-u)$ in front of the tensor $L_3^{\mu\nu}$ is chosen so as to make all five amplitudes F_i even under pion and photon crossing symmetry ($t \leftrightarrow u$) [21, 24]. We note that the Born terms possess a double pole structure in the soft-photon limit,

as a manifestation of Low's theorem [25]. The kinematic constraints can be obtained by analyzing projected helicity amplitudes in terms of the quantities

$$A_n^J(s) = \frac{1}{(pq)^J} \int_{-1}^1 \frac{dz}{2} P_J(z) F_n(s, t), \quad (5)$$

which are free of any singularities due to the properties of the Legendre polynomials [20]. In Eq. (5), q and p are initial and final relative momenta in the c.m. frame. Due to specifics of our basis (4), all of the results below are given for the Born subtracted p.w. amplitudes

$$\bar{h}_{\lambda_1\lambda_2}^{(J)} \equiv h_{\lambda_1\lambda_2}^{(J)} - h_{\lambda_1\lambda_2}^{(J), \text{Born}}, \quad (6)$$

where for s -wave it holds that [11]

$$\begin{aligned} \bar{h}_{++}^{(0)}(s) \pm \bar{h}_{00}^{(0)}(s) &\sim (s - s_{\text{kin}}^{(\mp)}), \\ s_{\text{kin}}^{(\pm)} &\equiv -(Q_1 \pm Q_2)^2, \end{aligned} \quad (7)$$

with $Q_i \equiv \sqrt{Q_i^2}$ ($i = 1, 2$). Note that in the single virtual and real photon cases these constraints are required by the soft-photon theorem [25] and have been implemented already in [24, 26, 27]. The kinematically uncorrelated amplitudes for the s -wave can be obtained by dividing the left-hand side (lhs) of Eq. (7) by its right-hand side (rhs)

$$\bar{h}_{i=1,2}^{(0)}(s) = \frac{\bar{h}_{++}^{(0)}(s) \pm \bar{h}_{00}^{(0)}(s)}{s - s_{\text{kin}}^{(\mp)}}. \quad (8)$$

In [17] the kinematically unconstrained basis of the partial wave amplitudes were derived for the single virtual case. Below we extend this result for the double-virtual case for $J = 2$,

$$\begin{aligned} (s + Q_1^2 + Q_2^2) \bar{h}_{+-}^{(2)} + 2\sqrt{2} Q_1^2 Q_2^2 \bar{h}_- &\sim \gamma_1(s), \\ \sqrt{2} \bar{h}_{+-}^{(2)} - \bar{h}_+ + (Q_1^2 + Q_2^2) \bar{h}_- &\sim \gamma_1(s), \\ \sqrt{2} \bar{h}_{+-}^{(2)} + (s + Q_1^2 + Q_2^2) \bar{h}_- &\sim \gamma_1(s), \\ \sqrt{6} s \bar{h}_{+-}^{(2)} - 2\sqrt{3} s \bar{h}_+ + 3s (s + Q_1^2 + Q_2^2) \bar{h}_0 &+ 6s \bar{h}_{++}^{(2)} \\ &+ \sqrt{3} (s^2 + 2(Q_1^2 + Q_2^2) s - (Q_1^2 - Q_2^2)^2) \bar{h}_- \sim \gamma_2(s), \\ 6s (s + Q_1^2 + Q_2^2) \bar{h}_{++}^{(2)} + 12 Q_1^2 Q_2^2 s \bar{h}_0 & \\ - \sqrt{6} (s(Q_1^2 + Q_2^2) + (Q_1^2 - Q_2^2)^2) \bar{h}_{+-}^{(2)} & \\ + 2\sqrt{3} (s(Q_1^2 + Q_2^2) + (Q_1^2 - Q_2^2)^2) \bar{h}_+ & \\ - 2\sqrt{3} (Q_1^2 - Q_2^2)^2 (s + Q_1^2 + Q_2^2) \bar{h}_- &\sim \gamma_2(s), \end{aligned} \quad (9)$$

with

$$\gamma_n(s) \equiv \lambda^n(s, -Q_1^2, -Q_2^2) (s - 4m_\pi^2), \quad (10)$$

where λ is the Källén triangle function and $\bar{h}_{+,-,0}$ were

introduced for convenience

$$\begin{aligned}\bar{h}_+(s) &\equiv \frac{\sqrt{s}}{Q_2} \bar{h}_{+0}^{(2)}(s) + \frac{\sqrt{s}}{Q_1} \bar{h}_{0+}^{(2)}(s), \\ \bar{h}_-(s) &\equiv \left(\frac{\sqrt{s}}{Q_2} \bar{h}_{+0}^{(2)}(s) - \frac{\sqrt{s}}{Q_1} \bar{h}_{0+}^{(2)}(s) \right) \frac{1}{Q_1^2 - Q_2^2}, \\ \bar{h}_0(s) &\equiv \frac{\bar{h}_{00}^{(2)}(s)}{Q_1 Q_2}.\end{aligned}\quad (11)$$

We emphasize, that in addition to the $s_{\text{kin}}^{(\pm)}$ points, the p.w. amplitudes for $J \neq 0$ exhibit a so-called centrifugal barrier factor at $4m_\pi^2$. The new set of amplitudes $\bar{h}_{i=1..5}^{(2)}(s)$ we obtain as in (8) by dividing the lhs of Eq. (9) by its rhs.¹ We emphasize that Eq. (9) shows the correlation of the p.w. helicity amplitudes explicitly, as compared with the result based on the Roy-Steiner equations [18, 28], where kinematic constraints are contained in the integral kernels. The full set of these off-diagonal kernels is given in [18], and the final solution is obtained by diagonalization of the kernel matrix.

B. Dispersion relations

The new set of amplitudes $\bar{h}_{1-5}^{(J)}$ contains only dynamical singularities. These are right and left-hand cuts, and one can write a dispersion relation in the following form (modulo subtractions which will be discussed in Section III)

$$\bar{h}_i^{(J)}(s) = \int_{-\infty}^0 \frac{ds'}{\pi} \frac{\text{Disc} \bar{h}_i^{(J)}(s')}{s' - s} + \int_{4m_\pi^2}^{\infty} \frac{ds'}{\pi} \frac{\text{Disc} h_i^{(J)}(s')}{s' - s}, \quad (12)$$

where we noted that $\text{Disc} \bar{h}_i^{(J)}(s) = \text{Disc} h_i^{(J)}(s)$ along the right-hand cut. The latter is determined by the unitarity condition and in the elastic approximation is given by

$$\begin{aligned}\text{Disc} h_i^{(J)}(s) &= t^{(J)*}(s) \rho(s) h_i^{(J)}(s), \\ \rho(s) &= \frac{p(s)}{8\pi\sqrt{s}} \theta(s - 4m_\pi^2),\end{aligned}\quad (13)$$

where $\rho(s)$ is a two-body phase space factor and $t^{(J)}(s)$ is the hadronic scattering amplitude, which is normalized as $\text{Im}(t^{(J)})^{-1} = -\rho$. For the energy region above 1 GeV, it is necessary to take into account the inelasticity. The first relevant inelastic channel is $K\bar{K}$, which is

required to capture the dynamics of the $f_0(980)$ scalar meson. For the coupled-channel case, the phase-space function $\rho(s)$ and the amplitude $t^{(J)}(s)$ turn into (2×2) matrices, while $h_i^{(J)}$ will be written in the (2×1) form with elements $h_i^{(J)}$ and $k_i^{(J)}$ which correspond to the $\gamma^* \gamma^* \rightarrow \pi\pi$ and $\gamma^* \gamma^* \rightarrow K\bar{K}$ amplitudes, respectively. The solution to Eq. (12) is given by the well known Muskhelishvili-Omnès method for treating the final-state interactions [29]. It is based on writing a dispersion relation for $\bar{h}_i^{(J)}(\Omega^{(J)})^{-1}$ [13], where $\Omega^{(J)}$ is the Omnès function which satisfies a similar unitarity constraint,

$$\text{Disc} \Omega^{(J)}(s) = t^{(J)}(s) \rho(s) \Omega^{(J)*}(s). \quad (14)$$

As a result, we obtain

$$\begin{aligned}h_i^{(J)}(s) &= h_i^{(J),\text{Born}}(s) \\ &+ \Omega^{(J)}(s) \left[- \int_{4m_\pi^2}^{\infty} \frac{ds'}{\pi} \frac{\text{Disc}(\Omega^{(J)}(s'))^{-1} h_i^{(J),\text{Born}}(s')}{s' - s} \right. \\ &\left. + \int_{-\infty}^0 \frac{ds'}{\pi} \frac{(\Omega^{(J)}(s'))^{-1} \text{Disc} \bar{h}_i^{(J)}(s')}{s' - s} \right],\end{aligned}\quad (15)$$

which can be straightforwardly generalized for the coupled-channel case. The Born subtracted amplitudes along the left-hand cut (the second term inside the brackets) are given by multi-pion exchanges in the t and u channels, which in practice can be approximated by resonance (R) exchanges [13]. The dominant contribution is generated by vector mesons ω and ρ . The contribution from other heavier resonances will be absorbed in an effective way by allowing for a slight adjustment of the $VP\gamma$ coupling [17].

Here we note that there is freedom in writing the dispersion relation. In principle, one could write a dispersion relation for the combination $(\bar{h}_i^{(J)} - h_i^{(J),V})(\Omega^{(J)})^{-1}$, as was done for $\gamma\gamma^* \rightarrow \pi\pi$ in [24]. However, in this case, one needs to make an assumption about the high-energy dependence of the real part of $h_i^{(J),V}$, as was explained in [18]. In this work, we take out only the Born term in Eq. (15) and therefore need to know only the high energy behavior of the imaginary part of the vector mesons exchange entering the left-hand cut, which does not have any polynomial ambiguity [13].

C. Left-hand cuts

The generalization of the Born contribution to the case of off-shell photons is performed by multiplying the scalar QED result by the electromagnetic pion (kaon) form factors [21, 30] which lead to the following invariant ampli-

¹ Note that when $Q_1^2 = Q_2^2$ (and pions are in the final state), special care is required. In that case, $H_{+0} = -H_{0+}$, and only four Lorentz tensors in Eq. (4) are independent. Therefore, one needs to reshuffle Eq. (9) in such a way that only four amplitudes $\bar{h}_i^{(J)}$ survive. We checked that numerically the results for $Q_1^2 \approx Q_2^2$ given by Eq. (9) are consistent with the strict $Q_1^2 = Q_2^2$ limit.

tudes

$$\begin{aligned}
F_1^{\text{Born}} &= -\frac{e^2 (4m_i^2 + Q_1^2 + Q_2^2)}{(t - m_i^2)(u - m_i^2)} f_i(Q_1^2) f_i(Q_2^2), \quad (16) \\
F_2^{\text{Born}} &= -\frac{e^2}{(t - m_i^2)(u - m_i^2)} f_i(Q_1^2) f_i(Q_2^2), \\
F_3^{\text{Born}} &= F_4^{\text{Born}} = F_5^{\text{Born}} = 0,
\end{aligned}$$

where $i = \pi (K)$ for $\gamma^* \gamma^* \rightarrow \pi\pi (K\bar{K})$. As these Born terms coincide with the pion pole terms obtained in a dispersive derivation, there is full agreement between the results of [21, 30]. We note that the double pole structure of the Born amplitudes does not bring extra complications to Eq. (15) since its singularities lie outside the physical region. The electromagnetic spacelike pion and kaon form factors in the region $Q^2 \lesssim 1 \text{ GeV}^2$ are parameterized by simple monopole forms yielding the following mass parameters: $\Lambda_\pi = 0.727(5) \text{ GeV}$ and $\Lambda_K = 0.872(47) \text{ GeV}$ with $\chi^2/\text{d.o.f.} = 1.22$ [31] and $\chi^2/\text{d.o.f.} = 0.69$ [32], respectively.

The vector-meson exchange left-hand cuts are obtained by the effective Lagrangian which couples photon, vector (V), and pseudoscalar (P) meson fields,

$$\mathcal{L}_{VP\gamma} = e C_{VP\gamma} \epsilon^{\mu\nu\alpha\beta} F_{\mu\nu} \partial_\alpha P V_\beta, \quad (17)$$

where $F_{\mu\nu} = \partial_\mu A_\nu - \partial_\nu A_\mu$. This Lagrangian density implies

$$\begin{aligned}
F_1^{V\text{exch}} &= -\sum_V \frac{e^2 C_{VP\gamma}^2}{2} \left(\frac{4t + Q_1^2 + Q_2^2}{t - m_V^2} + \frac{4u + Q_1^2 + Q_2^2}{u - m_V^2} \right) \tilde{f}_{V,i}(Q_1^2, Q_2^2), \quad (18) \\
F_2^{V\text{exch}} &= \sum_V \frac{e^2 C_{VP\gamma}^2}{2} \left(\frac{1}{t - m_V^2} + \frac{1}{u - m_V^2} \right) \tilde{f}_{V,i}(Q_1^2, Q_2^2), \\
F_3^{V\text{exch}} &= \sum_V \frac{e^2 C_{VP\gamma}^2}{2} \left(\frac{1}{u - m_V^2} - \frac{1}{t - m_V^2} \right) \tilde{f}_{V,i}(Q_1^2, Q_2^2), \\
F_4^{V\text{exch}} &= \sum_V e^2 C_{VP\gamma}^2 \left(\frac{1}{t - m_V^2} + \frac{1}{u - m_V^2} \right) \tilde{f}_{V,i}(Q_1^2, Q_2^2), \\
F_5^{V\text{exch}} &= 0, \\
\tilde{f}_{V,i}(Q_1^2, Q_2^2) &\equiv f_{V,i}(Q_1^2) f_{V,i}(Q_2^2),
\end{aligned}$$

where in the following we will use $g_{VP\gamma} \simeq C_{\rho^\pm, 0\pi^\pm, 0\gamma} \simeq C_{\omega\pi^0\gamma}/3$ as the only fit parameter, as discussed in [17], yielding $g_{VP\gamma} = 0.33 \text{ GeV}^{-1}$. This value lies within 10% with the Particle Data Group (PDG) average $g_{VP\gamma}^{\text{PDG}} = 0.37(2)$ [4], thus justifying the approximation of left-hand cuts by vector mesons. The slight difference accounts for the contribution from other heavier left-hand cuts, which in general should be taken into account by imposing Regge asymptotics. Such a study is, however, beyond the scope of this analysis. In Eq. (18) $f_{V,\pi}(Q_i^2)$ are vector meson transition form factors. For the ω , we use the dispersive analysis from [33] (see also [34]), while for the

ρ (sub-dominant) contribution we use the vector meson dominance model [35]. We note, that the form factors are well defined only for the pole contribution. Using the fixed- s Mandelstam representation, one can show that the vector pole contribution corresponds to replacing t and u with m_V^2 in the numerators of Eq. (18). This is different compared to Eq. (16), where the pion pole contribution coincides exactly with the Born contribution as discussed above. We emphasize that for the dispersion relations written in the form of Eq. (15) only $\text{Disc } h_{\lambda_1\lambda_2}^{(J),V}(s)$ is required as input, which is unique for the vector-pole contribution.

D. Analytic structure of the left-hand cuts

In order to find a solution of the dispersion relations given in Eq. (15), one needs to understand the singularity structure of the p.w. amplitudes $h_i^{(J)}$ as a function of the complex variable s . For space-like photons, the p.w. Born amplitudes are real functions above the threshold and do not bring any complexity. On the other hand, the vector-meson exchange left-hand cut is determined by four branching points: $s = 0$, $s = -\infty$, and

$$\begin{aligned}
s_L^{(\pm)} &= \frac{1}{2} (2m_\pi^2 - Q_1^2 - Q_2^2 - m_V^2 - \frac{(m_\pi^2 + Q_1^2)(m_\pi^2 + Q_2^2)}{m_V^2}) \\
&\pm \frac{\lambda^{1/2}(m_V^2, m_\pi^2, -Q_1^2) \lambda^{1/2}(m_V^2, m_\pi^2, -Q_2^2)}{2m_V^2}. \quad (19)
\end{aligned}$$

When one photon is real, the cut consists of two pieces: $(-\infty, s_L^{(-)})$ and $[s_L^{(+)}, 0]$. However, when both photons carry a space-like virtuality, one has to be careful since for $Q_1^2 Q_2^2 > (m_V^2 - m_\pi^2)^2$ the left-hand branch point $s_L^{(-)}$ moves to the right and reaches the pseudo-threshold point $s_{kin}^{(+)}$ and only then moves to the left (see Fig.1). In this case, the integration along the cut acquires an additional piece $[s_L^{(-)}, s_{kin}^{(+)}$], which is related to an "anomalous" discontinuity [36]. In addition, the integral around $s_{kin}^{(+)}$, in general, is nonzero and requires special care [18]. Indeed, according to Eq. (9), the $J = 2$ p.w. amplitude, that schematically is

$$h^V(s) = \frac{1}{(s - s_{kin}^{(+)})^2} \int_{-1}^1 \frac{z^4 dz}{t(s, z) - m_V^2}, \quad (20)$$

behaves like $(s - s_{kin}^{(+)})^{-9/2}$. Splitting the contour path into an integral up to $s_{kin}^{(+)} - \epsilon$ and a circular integral of radius ϵ around $s_{kin}^{(+)}$ (dashed curve in Fig.1) produces the cancellation of two singular pieces. In [18], this was solved by using a fit function (which consists of an appropriate square-root-like behavior and a polynomial) in the vicinity of the singular point. We follow here a different strategy and enlarge the contour around $s_{kin}^{(+)}$ such that one stays away from possible numerical issues related to

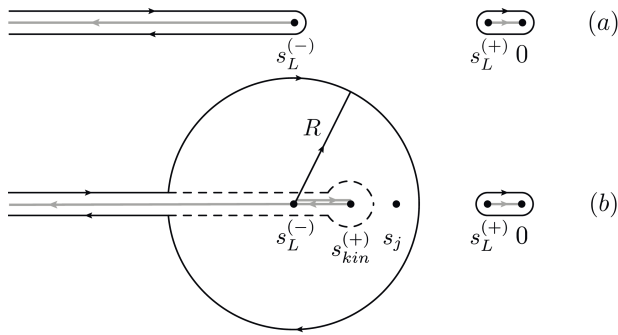


FIG. 1: Left-hand cut singularities and the integration contour for non-anomaly case (a) and its deformation for the anomaly case (b). See text for details.

the anomaly piece (see Fig.1). We propose to present $h^V(s)$ in the physical region as

$$h^V(s) = \int_{-\infty}^{s_L^{(-)}-R} \frac{ds' \text{Disc } h^V(s')}{\pi (s' - s)} + \int_{C_R} \frac{ds' h^V(s')}{2\pi i (s' - s)} + \int_{s_L^{(+)}}^0 \frac{ds' \text{Disc } h^V(s')}{\pi (s' - s)} \quad (21)$$

where R is chosen such that $s_j = -Q_1^2 - Q_2^2 + 2m_\pi^2 - 2m_V^2$ lies inside the circle. The location of s_j is determined by the condition that the imaginary part of the logarithm in Eq. (20) changes sign and therefore requires a proper choice of the Riemann sheet which we want to avoid. The merit of Eq. (21) is such that it works for both anomaly and non-anomaly cases, so one can use it for any space-like Q_i including the "transition" line when $Q_1^2 Q_2^2 = (m_V^2 - m_\pi^2)^2$. In addition, it is independent on the degree of singularity and can be used equally well for higher p.w. with $J > 2$. The generalization to the physical case with Omnès functions (15) is then straightforward since all of the quantities are well defined at complex energies.

For time-like virtualities (which are not of interest in this work) we refer the reader to [24, 37], where different cases of overlapping left- and right-hand cuts are considered.

E. Hadronic input

For the s -wave isospin $I = 0$ ($I = 2$) amplitude we use the coupled-channel (single channel) Omnès function from a dispersive summation scheme [19, 38] which implements constraints from analyticity and unitarity. The method is based on the N/D ansatz [39], where the set of coupled-channel (single channel) integral equations for the N -function are solved numerically with the input from the left-hand cuts which we present in a model-independent form as an expansion in a suitably constructed conformal mapping variable. These coefficients, in principle, can be matched to χ PT at low energy

[40]. Here we use a data-driven approach and determine these coefficients directly from fitting to Roy analyses for $\pi\pi \rightarrow \pi\pi$ [41], $\pi\pi \rightarrow K\bar{K}$ (for $I = 0$) [42], and existing experimental data for these channels. After solving the linear integral equation for $N(s)$, the D -function (the inverse of the Omnès function) is computed; more details will be given elsewhere [43].

For the d -wave $I = 0, 2$ amplitudes, we use the single-channel Omnès function in terms of the corresponding phase shifts,

$$\Omega_I^{(2)}(s) = \exp\left(\frac{s}{\pi} \int_{4m_\pi^2}^{\infty} \frac{ds' \delta_I^{(2)}(s')}{s' (s' - s)}\right). \quad (22)$$

Its numerical evaluation requires a high-energy parametrization of the phase shifts. We use a recent Roy analysis [41] below 1.42 GeV, and let the phase smoothly approach π (0) for $I = 0$ ($I = 2$) respectively.

III. DISCUSSION AND RESULTS

In Figs. 2 and 3, we plot the $\gamma^*\gamma^* \rightarrow \pi\pi$ cross sections which involve either two transverse (TT) photon polarizations or two longitudinal (LL) photon polarizations or one transverse and one longitudinal (TL) photon polarization defined by

$$\begin{aligned} \frac{d\sigma_{TT}}{d\cos\theta} &= \frac{\beta_{\pi\pi}}{64\pi\lambda^{1/2}(s, -Q_1^2, -Q_2^2)} (|H_{++}|^2 + |H_{+-}|^2), \\ \frac{d\sigma_{TL}}{d\cos\theta} &= \frac{\beta_{\pi\pi}}{32\pi\lambda^{1/2}(s, -Q_1^2, -Q_2^2)} |H_{+0}|^2, \\ \frac{d\sigma_{LL}}{d\cos\theta} &= \frac{\beta_{\pi\pi}}{32\pi\lambda^{1/2}(s, -Q_1^2, -Q_2^2)} |H_{00}|^2, \\ \beta_{\pi\pi} &= \frac{2p}{\sqrt{s}} \end{aligned} \quad (23)$$

where for the the neutral pions one has to include a symmetry factor of 1/2. The quantities σ_{TT} , σ_{TL} , σ_{LT} and σ_{LL} enter the cross section for the process $e^+e^- \rightarrow e^+e^-\pi\pi$ given in Refs. [44, 45]. It sets the convention for the flux factor, while the convention for the wave functions of the longitudinally polarized photons is chosen as

$$\begin{aligned} \epsilon^\mu(q_1, 0) &= \frac{1}{Q_1} (q, 0, 0, E_{q_1}), \\ \epsilon^\nu(q_2, 0) &= \frac{1}{Q_2} (-q, 0, 0, E_{q_2}), \\ E_{q_i} &= \sqrt{q^2 - Q_i^2}, \quad q = \frac{\lambda^{1/2}(s, -Q_1^2, -Q_2^2)}{2\sqrt{s}}. \end{aligned} \quad (24)$$

This convention reproduces continuously the real photon limit.

Using unsubtracted dispersion relations, we postdict the cross-sections for the real photon case and give predictions for finite virtualities. We implement rescattering in s - and d -waves, while the partial waves beyond are

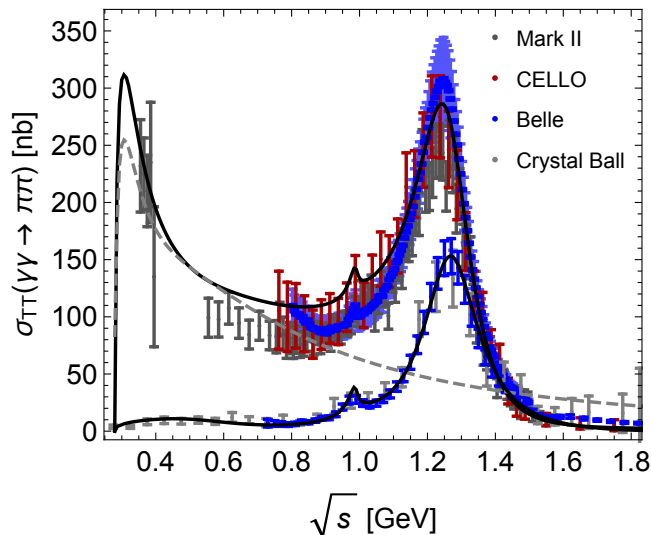


FIG. 2: Total cross sections for $\gamma\gamma \rightarrow \pi^+\pi^-$ ($|\cos\theta| < 0.6$) (upper curve) and $\gamma\gamma \rightarrow \pi^0\pi^0$ ($|\cos\theta| < 0.8$) (lower curve). The Born result is shown as dashed grey curves. The data are taken from [46].

approximated by the Born terms. Including Born left-hand cuts alone predicts a reasonable description of the $f_0(500)$ and $f_0(980)$ regions; however, it fails to describe the $f_2(1270)$ resonance. For the latter, the inclusion of heavier left-hands cuts is necessary [13]. Following our previous work [17], we approximate them with only vector meson exchanges and slightly adjust the coupling $g_{VP\gamma}$ in Eq.(18) to reproduce the $f_2(1270)$ peak in the $\gamma\gamma \rightarrow \pi^0\pi^0$ cross-section. We emphasize that this is the only parameter that we adjust to the real photon data to get a nice overall agreement (see Fig.2). We also note that the convergence of the unsubtracted dispersive integrals for $J = 2$ is, in general, better than for $J = 0$ due to the centrifugal barrier factor. Therefore, including vector meson left-hand cuts in the s -wave requires adding at least one subtraction, which can be fixed from chiral perturbation theory (χ PT). We checked that for relatively small Q^2 , the results of the two solutions are very similar. Since the finite Q^2 prediction from χ PT is expected to show large corrections for $Q^2 > 0.25 \text{ GeV}^2$, we decided to stay with the unsubtracted dispersion relation. In the present letter we show a selected result² for a fixed value $Q_1^2 = 0.5 \text{ GeV}^2$ for one photon virtuality and different values $Q_2^2 = 0.25, 0.5, 0.75, 1.0 \text{ GeV}^2$ for the second photon virtuality (see Fig.3). The last two Q_2^2 points are above the anomaly point. For σ_{TT} and σ_{LL} , we emphasize the importance of unitarization, which significantly

increases the pure Born prediction at low energy. For σ_{TL} , we notice that the helicity-1 contribution increases with increasing virtualities.

It is instructive to compare our approach with dispersive study based on the Roy-Steiner equations. In [18], there is a different strategy for treating kinematic singularities and anomalous thresholds. Second, there is a coupling between s -wave and d -wave with strength related to the high-energy behavior assumption. Third, the extra subtraction in [18] leads to a $1/s$ singular behavior, which is due to the truncation of the p.w. expansion. In our approach, we solve a p.w. dispersion relation under the assumption of maximal analyticity. For the s -wave (d -wave), we perform a coupled-channel (single channel) dispersive analysis and present a simpler implementation of the anomalous thresholds. Furthermore, in this approach, there is no coupling between s - and d -waves and no extra $1/s$ singularities. In a work in preparation [47], the comparison between [18] and our previous single virtual study [17] together with current work has been done. Both approaches agree well up to the details due to a different treatment of the vector-meson couplings, form factors, and the inclusion of the coupled-channel in the s -wave.

IV. CONCLUSION

In this work, we presented a dispersive analysis of the $\gamma^*\gamma^* \rightarrow \pi\pi$ reaction from the threshold up to 1.5 GeV in the $\pi\pi$ invariant mass. For the s -wave, we used a coupled-channel dispersive approach in order to simultaneously describe the scalar $f_0(500)$ and $f_0(980)$ resonances, while for the d -wave a single channel Omnès approach was adopted. The obtained results will serve as one of the relevant inputs to constrain the hadronic piece of the light-by-light scattering contribution to the muon's a_μ [11, 12]. Specifically it allows one to estimate the contributions from $f_0(500)$, $f_0(980)$, and $f_2(1270)$ resonances. The latter can be compared with the narrow resonance result [8, 9].

There are still a few open issues before it can be implemented in a $(g-2)_\mu$ calculation. First, one needs to validate a current treatment of left-hand cuts by forthcoming BESIII data on the $\gamma\gamma^* \rightarrow \pi^+\pi^-$ and $\gamma\gamma^* \rightarrow \pi^0\pi^0$ reactions [48]. This is a prerequisite for a data-driven approach in quantifying the uncertainty of the HLBL contribution to a_μ . Second, for higher Q^2 , one has to incorporate constraints from perturbative QCD for the vector transition from factors $f_{V,\pi}(Q^2)$ which is the driving force governing the Q^2 dependence of the $f_2(1270)$ resonance [3]. This will be investigated in a future work.

Acknowledgements

This work was supported by the Deutsche Forschungsgemeinschaft (DFG, German Research Foundation), in

² The preliminary plots for $Q_1^2 = Q_2^2 = 0.5 \text{ GeV}^2$ shown in [3] suffered from a numerical instability in the calculation of one of the five dispersive integrals, which led to an overestimation of σ_{LL} in the $f_2(1270)$ region, leaving the predictions for σ_{TT} and σ_{TL} mainly unchanged.

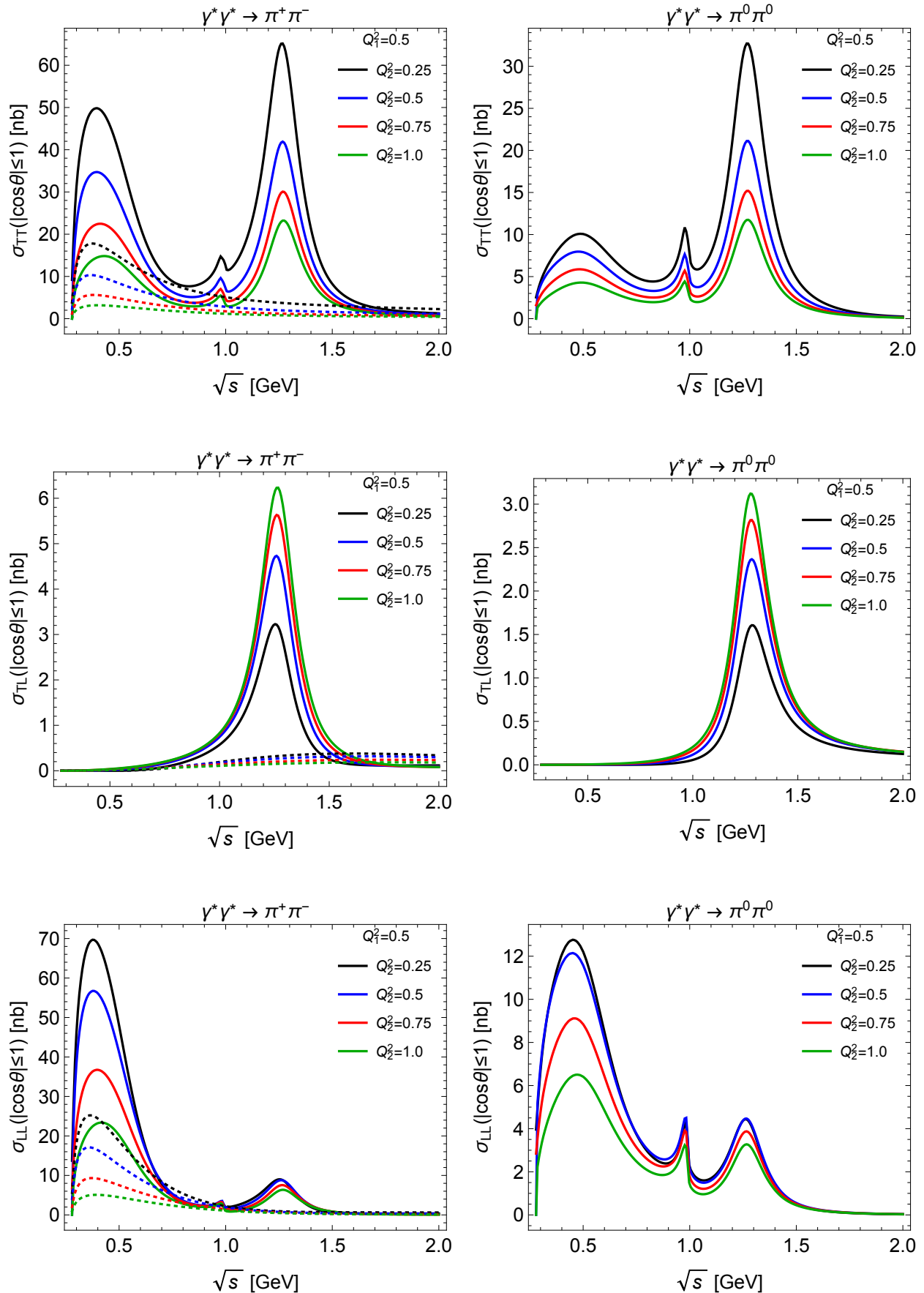


FIG. 3: Predictions for σ_{TT} , σ_{TL} , σ_{LL} cross sections for $\gamma^*\gamma^* \rightarrow \pi^+\pi^-$ (left panels) and $\gamma^*\gamma^* \rightarrow \pi^0\pi^0$ (right panels) for $Q_1^2 = 0.5$ GeV² and $Q_2^2 = 0.25, 0.5, 0.75, 1.0$ GeV² and for full angular coverage $|\cos\theta| \leq 1$. The Born results are shown as dotted curves.

part through the Collaborative Research Center [The Low-Energy Frontier of the Standard Model, Projekt-nummer 204404729 - SFB 1044], and in part through the Cluster of Excellence [Precision Physics, Fundamental

Interactions, and Structure of Matter] (PRISMA+ EXC 2118/1) within the German Excellence Strategy (Project ID 39083149). O.D. acknowledges funding from DAAD.

-
- [1] F. Jegerlehner, Springer Tracts Mod. Phys. **274**, pp.1 (2017).
- [2] A. Keshavarzi, D. Nomura, and T. Teubner, Phys. Rev. **D97**, 114025 (2018); M. Davier, A. Hoecker, B. Malaescu, and Z. Zhang, Eur. Phys. J. **C77**, 827 (2017), 1706.09436.
- [3] I. Danilkin, C. F. Redmer, and M. Vanderhaeghen, Prog. Part. Nucl. Phys. **107**, 20 (2019).
- [4] M. Tanabashi et al. (Particle Data Group), Phys. Rev. **D98**, 030001 (2018).
- [5] B. Lee Roberts (Fermilab P989), Nucl. Phys. Proc. Suppl. **218**, 237 (2011); J. Grange et al., arXiv:1501.06858 (2015).
- [6] H. Inuma (J-PARC muon g-2/EDM), J. Phys. Conf. Ser. **295**, 012032 (2011).
- [7] S. C. Frautschi, Regge poles and S-matrix theory, Frontiers in physics, W.A. Benjamin (1963).
- [8] V. Pauk and M. Vanderhaeghen, Eur. Phys. J. **C74**, 3008 (2014).
- [9] I. Danilkin and M. Vanderhaeghen, Phys. Rev. **D95**, 014019 (2017).
- [10] M. Masuda et al. (Belle), Phys. Rev. **D93**, 032003 (2016).
- [11] G. Colangelo, M. Hoferichter, M. Procura, and P. Stoffer, JHEP **04**, 161 (2017); G. Colangelo, M. Hoferichter, M. Procura, and P. Stoffer, Phys. Rev. Lett. **118**, 232001 (2017); G. Colangelo, M. Hoferichter, B. Kubis, M. Procura, and P. Stoffer, Phys. Lett. **B738**, 6 (2014).
- [12] V. Pauk and M. Vanderhaeghen, Phys.Rev. **D90**, 113012 (2014).
- [13] R. Garcia-Martin and B. Moussallam, Eur.Phys.J. **C70**, 155 (2010).
- [14] S. Mandelstam, Phys. Rev. **115**, 1741 (1959).
- [15] W. A. Bardeen and W. K. Tung, Phys. Rev. **173**, 1423 (1968); R. Tarrach, Nuovo Cim. **A28**, 409 (1975); D. Drechsel, G. Knochlein, A. Yu. Korchin, A. Metz, and S. Scherer, Phys. Rev. **C57**, 941 (1998).
- [16] S. Mandelstam, Phys. Rev. **112**, 1344 (1958).
- [17] I. Danilkin and M. Vanderhaeghen, Phys. Lett. **B789**, 366 (2019).
- [18] M. Hoferichter and P. Stoffer, JHEP **07**, 073 (2019).
- [19] A. Gasparyan and M. F. M. Lutz, Nucl.Phys. **A848**, 126 (2010).
- [20] M. F. M. Lutz and I. Vidana, Eur.Phys.J. **A48**, 124 (2012); Y. Heo and M. F. M. Lutz, Eur. Phys. J. **A50**, 130 (2014).
- [21] G. Colangelo, M. Hoferichter, M. Procura, and P. Stoffer, JHEP **09**, 074 (2015).
- [22] I. V. Danilkin, M. F. M. Lutz, S. Leupold, and C. Ter-schlusen, Eur.Phys.J. **C73**, 2358 (2013).
- [23] I. Danilkin, O. Deineka, and M. Vanderhaeghen, Phys. Rev. **D96**, 114018 (2017); O. Deineka, I. Danilkin, and M. Vanderhaeghen, EPJ Web Conf. **199**, 02005 (2019), 1808.04117.
- [24] B. Moussallam, Eur.Phys.J. **C73**, 2539 (2013).
- [25] F. E. Low, Phys. Rev. **110**, 974 (1958).
- [26] M. Hoferichter, D. Phillips, and C. Schat, Eur.Phys.J. **C71**, 1743 (2011).
- [27] D. Morgan and M. R. Pennington, Z. Phys. **C37**, 431 (1988); L.-Y. Dai and M. R. Pennington, Phys. Rev. **D90**, 036004 (2014); L.-Y. Dai and M. R. Pennington, Phys. Lett. **B736**, 11 (2014).
- [28] G. Colangelo, M. Hoferichter, M. Procura, and P. Stoffer, JHEP **09**, 091 (2014).
- [29] R. Omnes, Nuovo Cim. **8**, 316 (1958).
- [30] H. W. Fearing and S. Scherer, Few Body Syst. **23**, 111 (1998).
- [31] E. Dally et al., Phys. Rev. **D24**, 1718 (1981); S. R. Amendolia et al., Phys. Lett. **146B**, 116 (1984); V. Tadevosyan et al., Phys. Rev. **C75**, 055205 (2007).
- [32] E. B. Dally et al., Phys. Rev. Lett. **45**, 232 (1980); S. R. Amendolia et al., Phys. Lett. **B178**, 435 (1986); M. Carmignotto et al., Phys. Rev. **C97**, 025204 (2018).
- [33] I. V. Danilkin et al., Phys. Rev. **D91**, 094029 (2015).
- [34] S. Schneider, B. Kubis, and F. Niecknig, Phys.Rev. **D86**, 054013 (2012).
- [35] J. J. Sakurai, Currents and Mesons, University of Chicago Press (1969).
- [36] R. Karplus, C. M. Sommerfield, and E. H. Wichmann, Phys. Rev. **111**, 1187 (1958); S. Mandelstam, Phys. Rev. Lett. **4**, 84 (1960).
- [37] M. Hoferichter, G. Colangelo, M. Procura, and P. Stoffer, Int.J.Mod.Phys.Conf.Ser. **35**, 1460400 (2014).
- [38] I. Danilkin, A. Gasparyan, and M. Lutz, Phys.Lett. **B697**, 147 (2011).
- [39] G. F. Chew and S. Mandelstam, Phys.Rev. **119**, 467 (1960).
- [40] I. V. Danilkin, L. I. R. Gil, and M. F. M. Lutz, Phys.Lett. **B703**, 504 (2011); I. Danilkin and M. Lutz, EPJ Web Conf. **37**, 08007 (2012).
- [41] R. Garcia-Martin, R. Kaminski, J. R. Pelaez, J. Ruiz de Elvira, and F. J. Yndurain, Phys.Rev. **D83**, 074004 (2011).
- [42] P. Buettiker, S. Descotes-Genon, and B. Moussallam, Eur.Phys.J. **C33**, 409 (2004); J. R. Pelaez and A. Rodas, Eur. Phys. J. **C78**, 897 (2018).
- [43] I. Danilkin, O. Deineka, and M. Vanderhaeghen, (to be published) (2020).
- [44] V. M. Budnev, I. F. Ginzburg, G. V. Meledin, and V. G. Serbo, Phys. Rept. **15**, 181 (1975).
- [45] V. Pascalutsa, V. Pauk, and M. Vanderhaeghen, Phys. Rev. **D85**, 116001 (2012).
- [46] T. Mori et al., J.Phys.Soc.Jap. **76**, 074102 (2007); S. Uehara et al., Phys.Rev. **D79**, 052009 (2009); J. Boyer et al., Phys.Rev. **D42**, 1350 (1990); H. Behrend et al., Z.Phys. **C56**, 381 (1992); H. Marsiske et al., Phys.Rev. **D41**, 3324 (1990).
- [47] J. Bijnens et al., white paper (to be published) (2020).
- [48] C. F. Redmer (BESIII), Nucl. Part. Phys. Proc. **287-288**, 99 (2017).